

Experimental study of cohesive sediment consolidation and resuspension identifies approaches for coastal restoration: Lake Lery, Louisiana

Edward L. Lo · Samuel J. Bentley Sr. · Kehui Xu

Received: 31 January 2014 / Accepted: 25 August 2014 / Published online: 10 September 2014
© Springer-Verlag Berlin Heidelberg 2014

Abstract The purpose of this study was to evaluate related processes of sediment consolidation and resuspension in a coastal basin and how these processes influence retention of fine sediment delivered by a river diversion. Sediment samples were collected from Lake Lery, a coastal receiving basin of the Caernarvon Diversion from the Mississippi River, Louisiana. Consolidation was tested for six initial sediment concentrations (14.0–105 kg m⁻³) in a settling column over 15-day periods. Mud erodibility was tested at seven shear stress regimes (0.01–0.60 Pa) using a dual-core Gust erosion microcosm system, on cores containing suspensions that consolidated for 1, 2, and 4 weeks. Consolidation rates were found to be inversely and exponentially related to initial suspension concentration, over concentrations ranging from fluid mud (10–200 kg m⁻³) to hydraulic dredge effluent. Consolidation is best predicted by a function consisting of two exponential terms and one asymptotic constant, describing rates of rapid initial and slower subsequent settling. Coupled resuspension and consolidation tests (concentrations of 20–21 kg m⁻³) show that shear stresses generating the highest turbidity peaks increase from ≤ 0.30 Pa after 2 weeks of consolidation to ≥ 0.45 Pa after 4 weeks, and this strengthening cannot be attributed solely to increasing sediment concentration over time. Comparison of measured erosion shear stresses with bed shear stresses typical of coastal lakes and

bays suggests that this degree of strengthening, if given time to occur, could increase the overall retention of fine sediments deposited on lake and bay floors.

Introduction

The current land area of the Mississippi River Delta (MRD) is declining due to the combined effects of global sea level rise, subsidence, coastal erosion, and reduced sediment delivery (Blum and Roberts 2009). This is the case for many other large river deltas worldwide (Syvitski et al. 2009). For the MRD, plans to conserve the remaining land area and create new land have been presented in Louisiana's 2012 Coastal Master Plan (LA CPRA 2012), hereafter referred to as the Master Plan 2012. This plan aims for the extensive and efficient usage of sediment (both mud and sand) supplied via man-made diversions of the Mississippi River, as well as land built from dredge effluent, mined from the river bed and other sources. Approximately 90% of the riverine load is suspended mud (Nittrouer et al. 2008; cf. grain size finer than 63 μm). Computational sediment-transport models are being used to predict land-building capacity of river-sediment diversions (Meselhe et al. 2012). To accurately portray erosion, deposition, and consolidation of muds, these models must be calibrated for properties of local sediments. However, such rheological and sedimentological measurements for local MRD mud erosion, deposition, and consolidation are currently lacking.

Within this general framework, the overall goal of this study is to explore processes of consolidation and resuspension of fine-grained sediment in Lake Lery (Fig. 1), a natural coastal basin in the MRD that receives diverted water and sediment from the Mississippi River. Specific objectives are (1) to experimentally determine consolidation rates for suspended sediments spanning the suspended-sediment

E. L. Lo · S. J. Bentley Sr. (✉)
Department of Geology & Geophysics, Louisiana State University,
Baton Rouge, LA 70803, USA
e-mail: sjb@lsu.edu

S. J. Bentley Sr. · K. Xu
Coastal Studies Institute, Louisiana State University, Baton Rouge,
LA 70803, USA

K. Xu
Department of Oceanography and Coastal Sciences, Louisiana State
University, Baton Rouge, LA 70803, USA

concentration (SSC) range of natural fluid muds (10–200 kg m⁻³; e.g., Kineke et al. 1996; McAnally et al. 2007; Pappenmeier et al. 2013) and hydraulic dredge effluents (Turner 1996), (2) to experimentally determine the time dependency of sediment erodibility at different stages of consolidation, and (3) to evaluate the effectiveness of a published model for mud erosion, deposition, and consolidation (Sanford 2008), with respect to these experimental results. This research should help improve the accuracy of predictions for land building via diversions of muddy Mississippi River sediments and, more broadly, should provide improvements in approaches to model coupled processes of mud consolidation and erosion.

Cohesive sediment consolidation and erodibility

Sediment behaves cohesively when ≥10% of the mass of sediment is composed of mud-sized mineral grains (Whitehouse et al. 2000). Numerous studies have identified three distinct stages of densification for mud suspensions and deposits. During early stages of mud deposition, flocs of mud-sized sediment particles sink at rates governed by properties of individual flocs; as sediments accumulate on and near the bed, sediment mass concentration increases, reaching the condition of hindered settling, when the combination of upward fluid flow (to offset downward floc movement) and floc–floc interactions reduces floc settling velocities below the velocities of individual flocs in clear water (Winterwerp 2002; Winterwerp and Van Kesteren 2004). The mass concentration at which flocs generally come in contact with one another (gelling concentration; Winterwerp and Van Kesteren 2004) marks the transition from hindered settling to self-weight consolidation, at which time effective strength begins to develop. Precise conditions for these stages vary according to local sediment conditions, but the data synthesis of Whitehouse et al. (2000) suggests a threshold of unhindered to hindered settling near mass concentrations of 1–10 kg m⁻³, and the initiation of self-weight consolidation near mass concentrations of 100–200 kg m⁻³. Quantitative models for coupling hindered settling and self-weight consolidation have been developed (e.g., Toorman and Berlamont 1993; Toorman 1996) that define explicit nonlinear functions for each of these processes. Simpler empirical formulations have also been developed that portray basic changes in consolidation state, but using simpler mathematical approaches (e.g., Boudreau and Bennett 1999; Sanford 2008).

As muddy sediments deposit from a uniform suspension, the vertical distribution of the solids volume fraction ϕ_s normally evolves over time from a constant vertical profile to a profile where ϕ_s increases downward toward an asymptotic value (ϕ_∞), as described by Mulsow et al. (1998):

$$\phi_s(z) = \phi_\infty - (\phi_\infty - \phi_{s0}) \exp(-kz) \quad (1)$$

where $\phi_s(z)$ is the surface solids volume fraction at depth z , ϕ_{s0} is the solids volume fraction at the sediment surface, and k is an empirical exponential coefficient.

Depositing sediments produce a bed for which the critical bed erosion shear stress τ_e is generally positively related to sediment mass concentration C_m (dry mass of sediment per unit volume of water plus sediment):

$$\tau_e = E1(C_m)^{E2} \quad (2)$$

where $E1$ and $E2$ are site-specific coefficients (Jepsen et al. 1997; Whitehouse et al. 2000). Erosion of the bed occurs when the shear stress from waves or/and currents (τ_0) exceeds τ_e . The solids volume fraction C_m is related to mass concentration by $\phi_s = 1 - (C_m/\rho_s)$, where ρ_s is grain density. The rate of erosion (kg m⁻² s⁻¹) is:

$$\frac{dm}{dt} = m_e(\tau_0 - \tau_e) \quad (3)$$

where m is mass, t is time, m_e is an empirical erosion constant, and excess shear stress is $\tau_0 - \tau_e$.

Although these basic concepts are broadly applicable—such as the deposition-consolidation-resuspension model of Sanford (2008), or the model for estuarine fluid-mud dynamics of Winterwerp (2002)—parameterization of related processes is site-specific, depending on the particular sedimentological properties of local sediments (cf. above references). As a result, local studies, such as this one, are required to more accurately parameterize models of diversion-fed land building by muddy sediments, as proposed in the Master Plan 2012.

Study area

Lake Lery (Fig. 1) is a shallow basin (1.5 m maximum depth) located in the Breton Sound coastal drainage basin, which covers 1,100 km² of fresh, saline, and brackish wetlands (Lane et al. 1999) on the southeastern Louisiana coast within the MRD. Surface sediments are modern but are underlain by deposits formed 2,000–3,000 years ago comprising part of the Plaquemines-St. Bernard delta complex (Roberts 1997). The Caernarvon Diversion from the Mississippi River provides most freshwater and sediment input into Lake Lery, via Big Mar (the initial receiving basin for the diversion, and former agricultural land reclamation project) and Bayou Mandeville (Fig. 1b). The Caernarvon Freshwater Diversion was opened in 1991 for salinity control and delivery of mineral sediments to the Breton Sound basin. The Caernarvon Diversion generally flows at <183 m³ s⁻¹ but was designed to accommodate discharge up to 226 m³ s⁻¹ (Lane et al. 1999; Wheelock 2003).

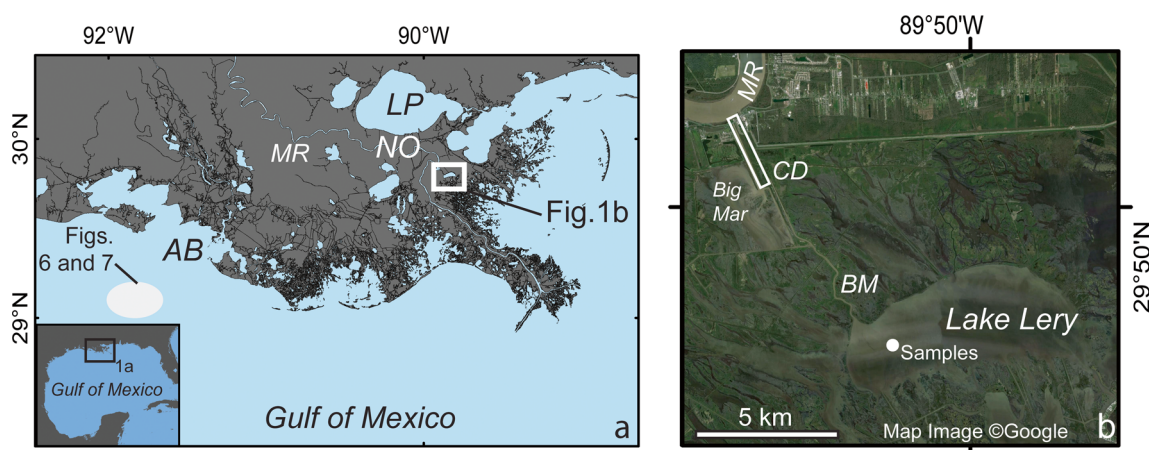


Fig. 1 Location of study area, with landmarks: **a** Lake Pontchartrain (LP), New Orleans (NO), Atchafalaya Bay (AB); *white ellipse* locations of Atchafalaya shelf samples shown in Figs. 5 and 6; **b** Mississippi River

(MR), Caernarvon Diversion (CD), Big Mar, Bayou Maurepas (BM), Lake Lery, and sediment sampling location (*white dot*)

Despite the low water and sediment discharge of the present diversion, $>5 \text{ km}^2$ of new land has been built in Big Mar during the past decade (Baker et al. 2011), and mineral sediment accumulation is also documented in surrounding wetlands (Lane et al. 1999; Wheelock 2003), presumably due to sediment delivered from the Caernarvon Diversion. The Master Plan 2012 proposes development of a much larger diversion (Upper Breton Diversion, flow capacity up to $7,000 \text{ m}^3 \text{ s}^{-1}$) at or near this site in the coming years. In addition, use of dredged Lake Lery sediments is proposed for marsh restoration projects in the near future (CWPPRA 2013). For these reasons, parameterization of depositional and erosional properties of these sediments is important for accurately predicting response of in situ and dredged sediments to waves and currents.

Materials and methods

Sediments were collected from the western end of Lake Lery, near the mouth of Bayou Mandeville in 1 m water depth (Fig. 1) using a Ponar grab sampler, and transported to laboratories at Louisiana State University. The sediment contained abundant large organic particulates. Because these particulates would interfere with testing apparatus and because the intent of the project was to study consolidation and erodibility of sediments similar to those delivered from the Caernarvon Diversion (i.e., more mineral content and less marsh debris), the collected mud was filtered through a 1-mm sieve to remove the particulates. Five subsamples of this homogenized sediment were wet-oxidized with hydrogen peroxide to remove organics, and analyzed for grain size using a Beckman-Coulter LS13-320 particle size analyzer. The material was then diluted sequentially with artificial seawater of 5 PSU (comparable to in situ salinity at the time of sediment

collection) to prepare six different suspensions for consolidation tests, with mass concentrations of 105, 54.7, 30.1, 22.8, 21.5, and 14.0 kg m^{-3} . Uncertainty in physical-property measurements was determined from the mean and standard deviation of five replicate analyses per suspension. These suspension mass concentrations were chosen to reflect a range from dredge effluent (mass concentration of 105 kg m^{-3}) that might be used for future marsh construction (cf. Turner 1996), to the more dilute fluid muds that can develop in bays receiving diversion flows (mass concentration of 14.0 kg m^{-3} ; e.g., Wax Lake Delta, Roberts 1997). Water delivered from the Mississippi is typically of lower sediment concentration ($<0.4 \text{ kg m}^{-3}$, Nittrouer et al. 2008), but such concentrations were too low to produce a deposited bed of sufficient thickness ($>10 \text{ cm}$) for resuspension tests using the methods described below. Consolidation of these suspensions was analyzed in a settling column, and one of the lower mass concentrations (22.8 kg m^{-3}) was chosen as nominal concentration for the time-series erodibility measurements.

For the highest and lowest suspension concentrations, mud was homogenized, and five aliquots were collected to assess water and organic content. Water content was determined gravimetrically by oven-drying samples at $100 \text{ }^\circ\text{C}$, accounting for salt content. Organic content was then determined by loss on ignition at $530 \text{ }^\circ\text{C}$ for 4 h (Heiri et al. 2001).

The settling column was adapted from designs of the US Army Corps of Engineers (US-ACE): 230 cm tall, diameter of 20.3 cm, with eight ball-valve sampling ports 1.25 cm in diameter, spaced at 20 cm intervals starting from 10 cm above the column base, and the top port at 160 cm above the base (US-ACE US-EPA 1998). For each consolidation test, sediment was mixed for 10 minutes using a commercial plaster mixer, and transferred to the settling column by means of a submersible pump and garden hose. During filling, a compressor-fed air hose was routed into the column to keep

the mixture homogenized during filling. Immediately following the pumping and removal of the air hose, one 50 mL sample of the sediment slurry was taken from each of the nine valves. This process was repeated 1, 3, 7, 13, 25, and 49 h later and at 48 h intervals after the 49th hour for a total duration of 15 days (as specified by US-ACE US-EPA 1998). External sections of the valve were flushed with water to clear each port of residual sediment. Within minutes of starting each experiment, clear water separated from the suspension to reveal a well-defined sediment surface; sediment height was measured immediately before and after each sampling event to enable correction of the height of the sediment column for volume lost during sampling. Elevation measurements were continued after the last sampling for most tests, for a total duration of up to 25 days. This process was repeated for six different experiments at the concentrations listed above.

Erodibility was tested with a dual-core Gust erosion microcosm system (GEMS; Gust and Muller 1997), which has been widely used for erodibility measurements at numerous sites along the US coastline (e.g., Dickhudt et al. 2009; Xu et al. 2014; Fig. 2). GEMS tests were conducted with a $\sim 20.9 \text{ kg m}^{-3}$ concentration (concentration within 10% of the 22.8 kg m^{-3} consolidation test).

To create a sediment column tall enough to allow deposition of a 10-cm sediment layer for GEMS tests, the 50-cm-long (10 cm diameter) GEMS core tube was extended vertically using an additional 200-cm tube, coupled with a flexible rubber connector. This enabled removal of the upper tube, after sediment deposited to form a layer in the lower tube for GEMS testing. Sediment preparation for erodibility

experiments was similar to that of the aforementioned consolidation experiments. At 1, 2, and 4 weeks after slurry introduction, the upper 200-cm tube (which contained clear water) was drained and removed carefully, and the lower 50-cm tube was used for erodibility measurements. Two cores were prepared for each settling period. Spinning disks at the top of a 10-cm column of water above the sediment–water interface generated seven shear stress levels: 0.01, 0.05, 0.10, 0.20, 0.30, 0.45, and 0.60 Pa (cf. Dickhudt et al. 2009). The cores were subjected to each shear stress level for 20 minutes in consecutive order from lowest to highest shear stress levels.

Toorman (1997) found that when a sudden step change in rotation speed is imposed, there is often oscillation of the solution due to the overshoot peak. When the change of the rotation speed is allowed to vary rapidly, but continuously over a small, finite period, the stress peaks reduce. In the present study, permanent shear with stepwise increased shear stress was used and the time steps were 20 minutes, which are much longer than the duration of oscillation due to overshoot peak (10s). This approach has been calibrated by Gust and Muller (1997) and widely used by Maa et al. (1998) for Baltimore Harbor, Stevens et al. (2007) in the Adriatic Sea, Law et al. (2008) in the Gulf of Lions, Dickhudt et al. (2011) in the York River of Chesapeake Bay, and Xu et al. (2014) on the Louisiana shelf.

The GEMS cores were connected to a pump that maintained water flow to extract the sediment that was suspended as a result of the applied shear stress (Fig. 2). Sediment concentration of the effluent was measured using two turbidimeters, and by filtration and gravimetric measurement of

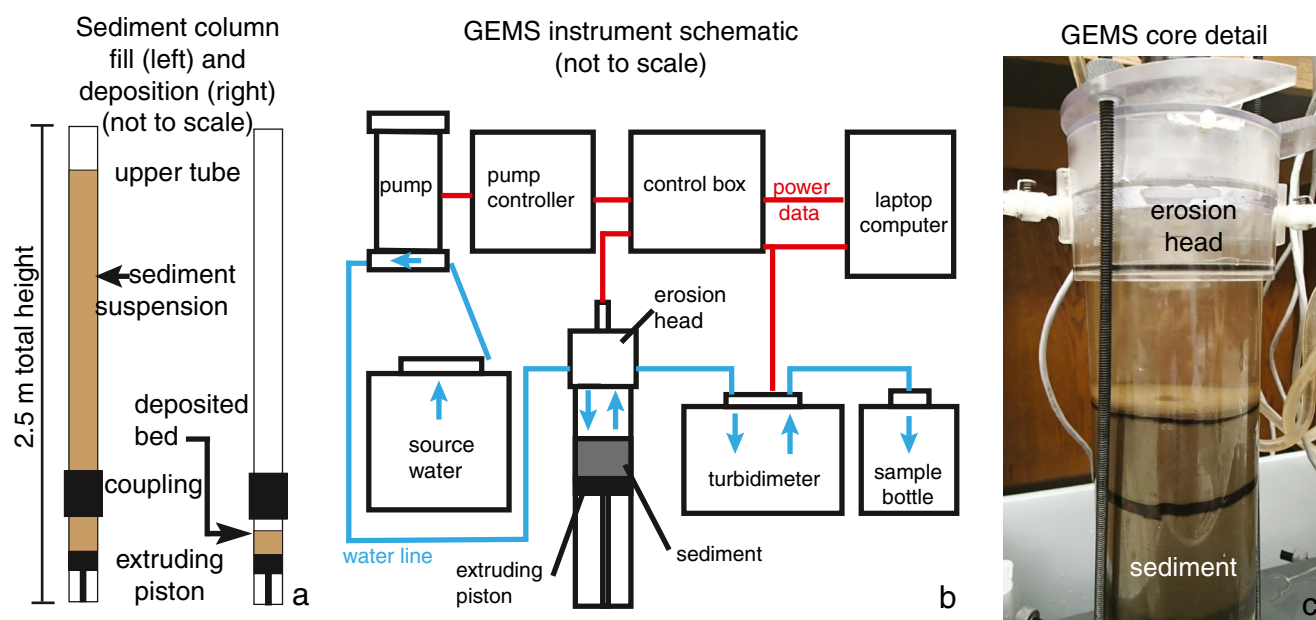


Fig. 2 **a** Schematic illustration of the settling columns used to prepare deposited sediments for testing. **b** Schematic of instruments and connections for the dual core GEMS; red lines electricity and data transfer, blue

lines water/sediment transfer connections. Modified from Green Eyes (2010). **c** Photograph of a GEMS tube showing sediment, erosion head, and transfer tubes for water and sediment

sediment content. This process was utilized to determine the amount of sediment eroded during each of the shear stress regimes. Tap water was used for the erodibility experiments, and was stored in buckets the day before experiments to ensure that a stable temperature was reached (about 21 °C). Control measurements of filter weights before and after tap water filtration indicated that background sediment concentration in the tap water was negligible. Accordingly, unlike the method of Dickhudt et al. (2009), eroded masses were calculated based on the weights of eroded sediment without subtracting background sediment mass.

Results

Physical properties of suspensions

The initial suspension that was diluted sequentially for all tests had the following physical properties: salinity 5 PSU, solids mass concentration $225 \pm 1.9 \text{ kg m}^{-3}$, organic content 18.2 $\pm 0.1\%$ by dry mass, solids volume fraction 0.092 ± 0.001 , and average solids density $2,440 \text{ kg m}^{-3}$, assuming organic-matter density of $1,500 \text{ kg m}^{-3}$. Initial suspension concentrations (C_0) for all settling column tests are shown in Table 1. The corresponding values for the suspension used for GEMS measurements are salinity 5 PSU, solids mass concentration $20.7 \pm 1.0 \text{ kg m}^{-3}$, organic content $14.6 \pm 0.5\%$ by dry mass, solids volume fraction 0.011 ± 0.0004 , and average solids density $2,480 \pm 10 \text{ kg m}^{-3}$.

The sediment used in all experiments contained 14–18% organic matter by dry mass. During the settling of sediment slurry, low-density organic matter appeared to settle slowly and accumulate on the sediment surface of GEMS cores. Within this organic-rich layer, a mat developed over time

during consolidation, but the mat was entirely eroded by the applied shear stresses during GEMS tests.

Consolidation tests

Time-series measurements of sediment mass concentration at each sampling port were produced for each initial concentration (Fig. 3a, b, Table 1). The initial concentrations for all tests fall in the range of likely hindered settling (Whitehouse et al. 2000). In testing the highest initial concentration (Fig. 3a), the effects of stratification were seen in the curvature of the individual plots taken at each sampling period. During the first 48 h, the concentration decreased with depth within a single sampling period except at 10 cm elevation, which had a higher concentration than observed at 30 cm elevation. In tests with lower initial sediment concentrations, the concentration increased with depth at each measurement period (shown for 22.8 kg m^{-3} in Fig. 3b).

Evaluation of all consolidation tests showed that the rate at which the consolidating sediment bed decreased in height decreased with increasing initial concentration (Figs. 3 and 4). However, there was some variability within this trend. For example, in the case of an initial concentration of 105 kg m^{-3} (Fig. 3a), the sediment concentration increased with each successive time period. For samples collected at 7, 24, and 48 h, concentrations displayed mid-depth minima, indicating highest concentrations at top and bottom. This effect was most clearly visible in the first few hours of the experiment and no longer readily apparent by 96 h.

In Fig. 4 (cf. Table 2), sediment surface height (normalized to initial height for each test) was compared for all six settling column tests. The rate of decrease in sediment surface height was most rapid for lowest initial concentrations, more quickly

Table 1 Initial concentration of solids C_0 (kg m^{-3}) from each of the nine valves of the settling tube at time $t=0$ for the six tests, with average values (Avg.) and standard deviations (SD). Samples were collected within the

Valve outlet	Height from top (cm)	Height from bottom (cm)	Test 1	Test 2	Test 3	Test 4	Test 5	Test 6
Init. conc. (kg m^{-3})			105.0	14.0	54.7	30.1	21.5	22.8
0-1	–190.5	10.5	104.0	16.1	55.6	42.2	23.3	24.5
0-2	–170.5	29.5	103.0	14.8	55.1	38.0	21.9	23.1
0-3	–150.5	49.5	105.0	14.4	54.2	23.8	21.3	22.4
0-4	–130.5	69.5	105.0	13.3	54.7	28.5	21.7	23.2
0-5	–110.5	89.5	105.0	13.9	54.8	27.9	21.6	22.4
0-6	–90.5	109.5	104.0	13.3	54.1	29.4	20.6	22.9
0-7	–70.5	129.5	105.0	14.0	54.9	28.0	21.3	22.9
0-8	–50.5	149.5	105.0	12.9	54.6	26.2	20.7	21.9
0-9	–40.5	159.5	106.0	13.0	54.1	27.2	20.6	22.3
Avg.			105.0	14.0	54.7	30.1	21.5	22.8
SD			0.7	1.0	0.5	6.0	0.9	0.8

first 5 minutes of deactivating the air hose that had maintained a well-homogenized suspension; small deviations from C_0 showed that settling had already commenced

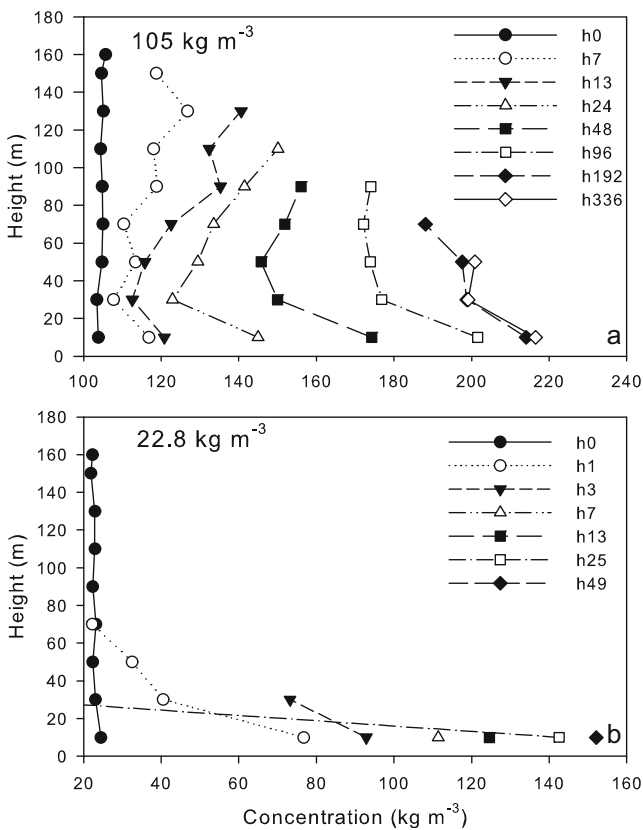


Fig. 3 **a** Time series of suspension dry bulk density with $C_0=105 \text{ kg m}^{-3}$ where the height of the sediment suspension decreases over time (hours 0, 7 . . . 336 of the experiment) as the sediment concentration within the settling column increases. **b** Corresponding time series for $C_0=22.8 \text{ kg m}^{-3}$

approaching an asymptotic elevation for each test than for the highest concentrations.

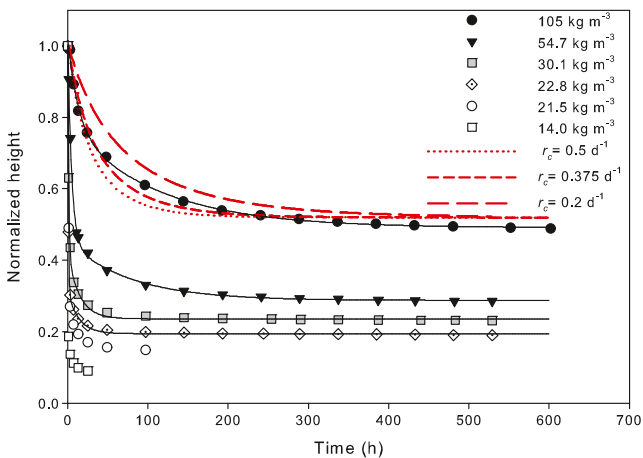


Fig. 4 Composite plot of normalized sediment suspension height vs. time for each of the six settling column experiments (scatter plots labeled by initial concentration) with regressions of Eq. 4 plotted as lines for tests exceeding 500 h in duration. In each case, $r^2=0.99$. Coefficient values for each regression are shown in Table 2. Red curves are results for the Sanford (2008) consolidation model, as described in text below, using a range of consolidation rates, and initial and boundary conditions for the 105 kg m^{-3} experiment. Sediment settles more rapidly in suspensions of lower concentration

Table 2 Parameters for regressions in Fig. 4, using Eq. 4

Parameter ^a	Test 1	Test 3	Test 4	Test 6
Init. conc. (kg m^{-3})	105.0	54.7	30.1	22.8
H_∞	0.491	0.288	0.236	0.195
a	0.239	0.554	0.582	0.690
b	0.078	0.214	0.917	1.359
c	0.286	0.165	0.180	0.116
d	0.009	0.013	0.068	0.072

^a Definitions: H_∞ , normalized asymptotic height after long consolidation; a and b , linear and exponential coefficient for early settling, respectively; c and d , linear and exponential coefficient for advanced consolidation, respectively

Comparing Fig. 3a and b, the concentration for the lowest sampling port in each test shows that tests beginning at higher C_0 reached a higher final concentration compared to lower C_0 . However, tests at lower C_0 reached asymptotic maximum concentrations earlier than for tests at higher C_0 .

To provide a simpler means of comparing consolidation time-scales for all six tests, the time for each test at which the sediment surface reached 50% of initial height was determined from each dataset (t_{50} , using linear interpolation if the elapsed time fell between measurement times; Table 3). These results are plotted against initial concentration (C_0) in Fig. 5, in a log-linear plot.

Erodibility experiments

The turbidity peaks generated during seven levels of shear stresses in GEMS tests varied greatly among experiments (Fig. 6). Duration and sequence of applied shear stresses in the GEMS experiments are shown in Fig. 6a, and timing and magnitude of sediment erosion are shown in Fig. 6b and c. For useful context, results of GEMS experiments for natural sediment cores from the Atchafalaya shelf (Fig. 1a; Xu et al. 2014) are shown in Fig. 6d. Composition and concentration of sediments used for erodibility experiments were most comparable to suspension concentrations of 21.5 and 22.8 kg m^{-3} used for consolidation tests. In the 1-

Table 3 Values of t_{50} (time needed for the normalized sediment height to reach 50% of its original height), as well as initial and final sediment mass concentration for the six tests (see Fig. 5)

Test	Init. conc. C_0 (kg m^{-3})	Final conc. C_t (kg m^{-3})	t_{50} (h)
1	105.0	214.0	408.0
2	14.0	155.0	0.4
3	54.7	192.0	~10.0
4	30.1	130.0	~2.0
5	21.5	144.0	1.0
6	22.8	120.0	0.9

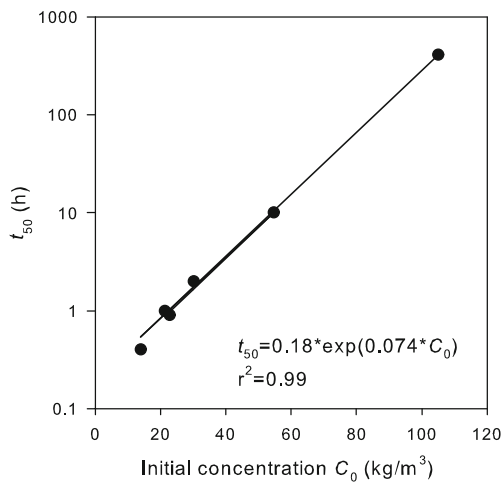
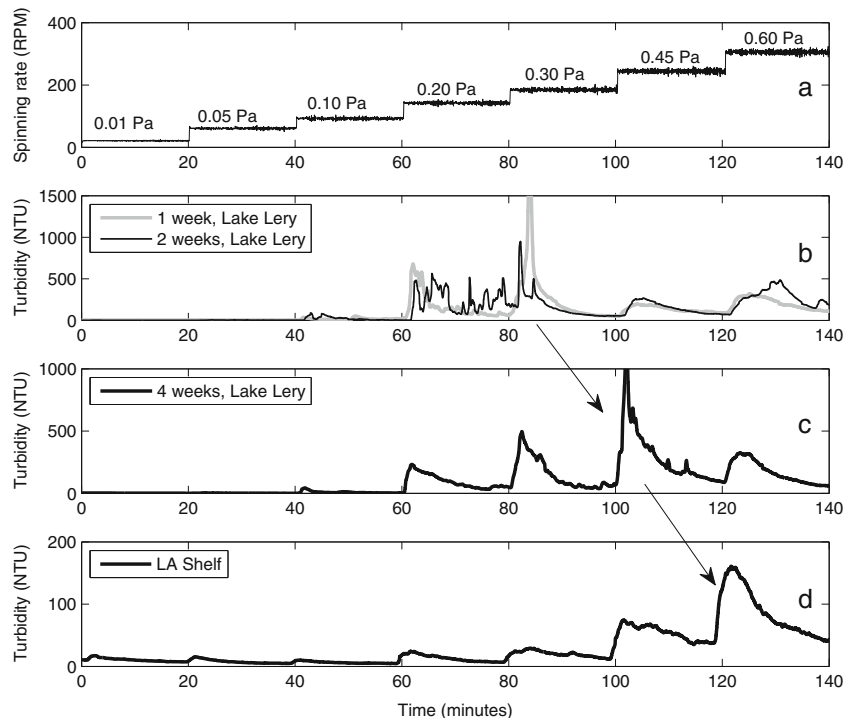


Fig. 5 Regression analysis of t_{50} (time required for the initial normalized height of the sediment suspension to reduce by half) vs. initial sediment concentration C_0 for all six consolidation tests, with evidence of a good positive relationship between these two parameters (for raw data, see Table 3). The line plot represents regression results for the exponential equation shown, with goodness of fit r^2

week experiment, no significant turbidity peak was found until a shear stress of 0.2 Pa was applied (Fig. 6b). Turbidity peaked at nearly 2,000 NTU (nephelometric turbidity units) when a shear stress of 0.3 Pa was applied, and this reading was the highest among all three experiments. The peak decreased to <300 NTU when shear stresses of 0.45 and 0.6 Pa were applied.

Fig. 6 Results of GEMS tests with Lake Lery and Louisiana shelf sediments: **a** spinning rate (RPM, revolutions per minute) and shear stress levels subjected to cores in all three consolidation periods; **b** turbidity changes for Lake Lery sediments after 1 and 2 weeks of consolidation; **c** turbidity trend for Lake Lery sediments after 4 weeks of consolidation; **d** turbidity trend for Louisiana shelf sediment (20 m water depth, south of Atchafalaya Bay; extracted from Xu et al. 2014). The shear stress generating maximum turbidity increases from 0.3 Pa in the 1- and 2-week Lake Lery tests, to 0.45 Pa for the 4-week Lake Lery test, and to 0.6 Pa for Louisiana shelf sediments (arrows)



For the 2-week GEMS test, erodibility for the first three shear stresses was similar to the 1-week test (Fig. 6b). Turbidity peaks were found at shear stresses of both 0.2 and 0.3 Pa, but the curve of the 2-week test was highly variable (Fig. 6b), with a lower turbidity peak at a shear stress of 0.3 Pa than was observed for the 1-week test. Turbidity peaks at shear stresses of 0.45 and 0.6 Pa were at levels similar to the 1-week test.

Sediment tested after 4 weeks appeared to have strengthened (Fig. 6c) more than sediment tested at 1 and 2 weeks. Comparison of turbidity curves in Fig. 6b and c showed a shift of the highest turbidity peaks from 0.3 Pa shear stress in 1- and 2-week experiments to 0.45 Pa shear stress in the 4-week experiment.

Cumulative eroded masses vs. shear stresses in each of the resuspension tests are shown in Fig. 7, and step-by-step eroded masses appear in Table 4, demonstrating that eroded mass generally decreased with increasing time allowed for consolidation. Specifically, for the 4-week test, the shear stress required to erode a cumulative mass of 0.2 kg m^{-2} was higher by $\sim 0.1 \text{ Pa}$ than for the tests of 1 and 2 weeks. For relevant comparison, average cumulative mass eroded from Louisiana continental shelf cores (Xu et al. 2014) is also shown in Fig. 7. A weak organic mat was observed to grow on the sediment surface in tubes prepared for each test period, although in each case the mat was removed by erosion before peak shear stresses were applied, so that

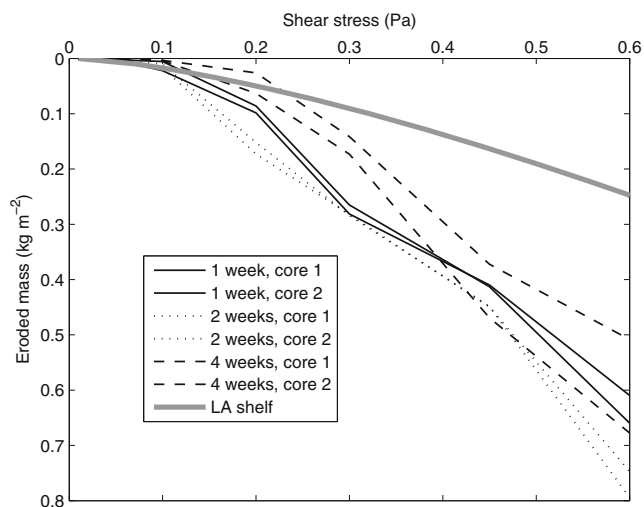


Fig. 7 Cumulative eroded mass vs. shear stress for all six Lake Lery sediment tests using the GEMS, along with average cumulative eroded mass for Louisiana shelf sediments (the latter extracted from Xu et al. 2014)

the highest shear stresses eroded mainly inorganic sediment, not organic mat material.

Turbidity (NTU) in GEMS tests was measured based on the optical properties of sediment particles using the turbidimeters, but eroded masses per unit area (kg m^{-2}) at given shear stresses can be used as an indicator of erodibility as well. For example, when 0.3 Pa shear stress was applied in GEMS tests, eroded mass was $\sim 0.28 \text{ kg m}^{-2}$ in 1- and 2-week experiments, but was only 0.15 kg m^{-2} in the 4-week experiment (Fig. 7).

Comparison of Figs. 4 and 7 showed that consolidation for at least 4 weeks was required for the freshly deposited sediment to reach critical shear strengths comparable to that of the nearby Louisiana continental shelf. Results in Fig. 4 indicate that consolidation for sediment of $20\text{--}22 \text{ kg m}^{-3}$ reached asymptotic values by 7 days (168 h), and did not change appreciably in average bulk density (based on the height of the sediment column) over the next 21 days. However, Table 4 and Fig. 7 demonstrate that measureable sediment strengthening with respect to erodibility occurred between 2 and 4 weeks.

Table 4 Total amount of sediment (in grams) eroded at each shear stress regime

Shear stress (Pa)	1 Week		2 Weeks		4 Weeks	
	Core 1	Core 2	Core 1	Core 2	Core 1	Core 2
0.01	0.0139	0.0082	0.0116	0.0058	0.0032	0.0064
0.05	0.0013	0.0108	0.0090	0.0087	0.0032	0.0039
0.10	0.0245	0.1400	0.0524	0.1040	0.0236	0.0138
0.20	0.5740	0.5420	1.0084	1.1100	0.4210	0.1620
0.30	1.2700	1.3000	0.9440	0.7760	0.7820	0.8220
0.45	1.0500	0.9160	1.1700	1.1900	2.1100	1.6400
0.60	1.7600	1.4200	2.4600	2.1200	1.4800	0.9710

Discussion

Consolidation tests

During consolidation tests, mid-depth minima in Fig. 3a could be the result of either air bubbles trapped in the sampled suspension, gravitational segregation of particles due to varying settling velocities of particles and aggregates, or non-uniform escape of pore waters from different levels, essentially blocking channels for water to escape from further below in the floc matrix. The latter two cases might have produced a zone of low density in the middle height of the column.

Figure 4 summarizes results for all tests in terms of normalized sediment height versus time. Sediment concentrations spanning the range of $20\text{--}220 \text{ kg m}^{-3}$ (Fig. 3) suggest that processes active in these experiments include both hindered settling and self-weight consolidation, similar to the study of Toorman and Berlamont (1993). If this is the case, then these sequential processes might best be represented mathematically by two separate rates of densification: the first for lower concentrations in which flocs settle but are not deformed (hindered settling), and the second for more strongly interacting flocs and aggregates (self-weight consolidation) at concentrations above the gelling concentration. To represent this, a regression analysis of suspension height versus time was conducted on results for the four tests that each ran for $>500 \text{ h}$ (22.8, 30.1, 54.7, and 105 kg m^{-3} , with regressions shown as solid-line plots in Fig. 4), using an equation with two separate exponential terms and an asymptotic constant:

$$H_t = H_\infty + ae^{(-bt)} + ce^{(-dt)} \tag{4}$$

where H_t is sediment height at time t , H_∞ is the asymptotic height after a long period of consolidation, a and b are the linear and exponential coefficients for early settling, and c and d are the linear and exponential coefficients for self-weight consolidation, respectively. This equation is conceptually similar to the Toorman and Berlamont (1993) consolidation model in terms of addressing both hindered settling and self-weight consolidation but is simpler mathematically. To evaluate bulk physical properties using this approach, average sediment concentration at time t (C_t) can be calculated from:

$$C_t = C_0(H_0/H_t) \tag{5}$$

where C_0 is initial concentration (Table 3), H_t is height at time t , and H_0 is initial height. In each case, $r^2=0.99$, demonstrating an excellent regression fit at each stage of densification (Fig. 4). These results supported the hypothesis that two separate consolidation processes with different rates contributed to the overall change in sediment-bed height and average sediment concentration.

This approach could be used to predict consolidation time-scales for natural and engineered deposits in this locale and potentially elsewhere. This prediction is possible because the higher concentration (e.g., 105 kg m^{-3}) is similar to those commonly reported for the effluent of dredging operations in the region and elsewhere (e.g., Palermo and Thackston 1988), widely used to construct marshlands such as those proposed for the Lake Lery shoreline in the near future (CWPPRA 2013). Likewise, the lower concentrations (e.g., $<22.8 \text{ kg m}^{-3}$) typify natural fluid mud deposits ($10\text{--}40 \text{ kg m}^{-3}$) that occur in river-influenced estuaries of the MRD (Roberts 1997) and worldwide (e.g., Weser estuary of the southern North Sea coast, Schrottke et al. 2006; for comprehensive review, see McAnally et al. 2007).

A regression analysis between C_0 and t_{50} in Fig. 5 was conducted using a simple exponential equation, resulting in $r^2=0.99$ (Fig. 7). These results suggest that the general consolidation rate is an exponential function of C_0 . Although this regression appears to describe overall mud behavior, regression fits for individual time series (Fig. 4) require two exponential terms and an asymptotic constant (Eq. 4) to capture the specific evolution of individual consolidation tests.

Sediment erodibility

The observed shift in highest peaks of SSC indicated that, as consolidation progressed, a higher shear stress was needed to suspend a significant amount of sediment off the water–sediment surface. Xu et al. (2014) conducted GEMS tests at sea for >100 sediment cores collected from the Louisiana shelf (mainly along 20-m isobaths; Fig. 1a), and reported that the highest peaks of SSC were mainly found at a shear stress level of 0.6 Pa. One representative turbidity curve can be seen in Fig. 6d. Sediment on the Louisiana shelf had probably rested undisturbed (with respect to resuspension) for longer time than the 1–4 week experiments in this study and were thereby more consolidated. Thus, it seems that the shear stress required to generate peak turbidity shifted from low (0.3 Pa) to high (0.6 Pa) levels of shear stresses when sediment became increasingly consolidated.

In the field measurements of Xu et al. (2014), on average only 0.08 kg m^{-2} of older sediment collected from the nearby shelf was eroded at 0.3 Pa shear stress under the same erodibility test conditions that were subjected to the cores in the GEMS tests (Fig. 6). This value was lower than that of the 4-week experiment (0.15 kg m^{-2} eroded), and the 1- and 2-week experiments ($\sim 0.28 \text{ kg m}^{-2}$ eroded). The increased strengthening observed in the 4-week experiment did not appear to be purely the result of decreasing water content over time. Sediment with C_0 of $20\text{--}22 \text{ kg m}^{-3}$ reached asymptotic values during the first week of consolidation, while erodibility tests demonstrated measureable sediment strengthening between 2 and 4 weeks. These data suggested that this strengthening was

probably through the bonds between flocs in the floc matrix over time, rather than increasing sediment bulk density.

The development of an organic mat was presumably due to microbial processes. This mat may have contributed to the reduced resuspension of sediment in 0.01, 0.05, and 0.1 Pa shear stresses in all three experiments (Fig. 6b and c). Once the mat was dispersed in the experiments, a substantial amount of sediment was eroded (Fig. 7). Although the presence of the organic mat may have lowered sediment resuspension at lower shear stresses, sediment erosion at the highest shear stresses was controlled by the consolidation state of the sediment, not the presence of a surficial organic mat. It is unlikely that natural in situ lake sediments, stirred by waves and currents and bioturbated by local fauna, would develop such a microbial mat under field conditions; however, in restricted basins, such as nearby marsh interiors that experience temperature and salinity extremes, such microbial mat development is plausible (for useful review, see Franks and Stolz 2009).

In the present study, the modest increases in erosion shear stress from 1 to 4 weeks shown by the experiments might suffice to increase the retention of muddy sediments delivered to coastal lakes and bays, if sufficient time were available for strengthening to occur. These results can be compared with bed shear stresses typical of Louisiana coastal lakes and bays under fair-weather and cold-front conditions (Moeller et al. 1993). Under commonly occurring cold-front winds of 10 m s^{-1} blowing across an 8 km fetch in water 4 m deep (characteristic of larger coastal Louisiana bays), typical wave properties (limited by fetch and depth) can be estimated using simple methods from the US-ACE (2002), yielding wave height and period of $\sim 0.45 \text{ m}$ and 2.0 s , respectively. Bed shear stress estimated from these waves and linear wave theory (Wright 1995) yields a range of $0.01\text{--}0.4 \text{ Pa}$ in water shoaling from 4 to 1.5 m depth. These results suggest that the strengthening that occurred during 4 weeks of consolidation may be sufficient to increase shear stress for erosion above values typical of most fair-weather and cold-front conditions, especially in areas of coastal bays deeper than 1.5 m, or bays with shorter fetch, smaller waves, and less resuspension. Because passage of cold fronts during fall, winter, and spring in the region routinely occurs every 3–7 days (Kineke et al. 2006), natural resuspension of these deposits is likely, unless sheltered in more quiescent natural or engineered settings. In other words, engineering designs to reduce such wave resuspension would be one approach to enhancing fine-sediment retention in diversion-receiving basins.

Integrating sediment consolidation and erodibility

The consolidation/erosion model of Sanford (2008) was evaluated using experimental data from the present study to predict consolidation profiles so as to facilitate predictions of both consolidation and erodibility allowed by the model.

The model was initialized and calibrated for the 105 kg m^{-3} test using the methods described by Sanford (2008): initial conditions were set by initial sediment height and concentration, and the sediment column height and solids volume fraction at $t=\infty$ were determined by a fit of Eq. 1 to sediment column data for the final sampling event. In Fig. 4, red dashed/dotted curves illustrate model results in terms of normalized height of the sediment column, using a range of values for the consolidation rate r_c (day^{-1} , in Eq. 2 of Sanford 2008), which is the only adjustable coefficient in the model controlling sediment height and concentration profiles. These results demonstrate that the existing Sanford (2008) formulation underestimates sediment column height after settlement for times >250 h, with better success at replicating experimental results over shorter timescales. For the test case presented by Sanford (2008), his consolidation model performed well and was evaluated over timescales <168 h. This suggests that the approach of using a single exponential consolidation rate can adequately simulate either early stages of settlement (hindered settling and the transition into self-weight consolidation) or later stages (primarily self-weight consolidation), but not both.

The Sanford (2008) model has the advantage of combining relatively realistic, empirical representations of mud erosion and consolidation, without producing high computational burdens, and shares the same approach to modeling consolidation and erosion as the SedTrans05 model of Neumeier et al. (2008). Although these two models lack the explicit treatment of elements such as gelling, or floc development and breakup found in more complex models such as that of Winterwerp (2002), they have the advantage of computational efficiency. As a result, consolidation/erosion algorithms similar to those of Sanford (2008) are becoming widely used in modeling cohesive sediment transport and deposition (e.g., Rinehimer et al. 2008; Gong and Shen 2009; Amoudry and Souza 2011; Fall et al. 2014). A potentially productive area for future research in muddy sediment dynamics might be development of more broadly accurate (but not overly complex) formulations (perhaps similar to Eq. 4), while maintaining the computational merits of the existing model (Sanford 2008). Such models, coupled with standardized experimental tests for consolidation and erodibility, would enhance our ability to predict the coupled evolution of muddy sediment consolidation and critical shear stress.

Conclusions

The primary conclusions of this study are as follows:

1. Sediments from Lake Lery displayed consolidation rates that appeared to be inversely and exponentially related to initial concentrations C_0 , over a range of concentrations ($14\text{--}105 \text{ kg m}^{-3}$) equivalent to the range from fluid mud to hydraulic dredge effluent used for marsh restoration of coastal Louisiana.
2. Consolidation for suspension tests was best predicted by a function consisting of two exponential terms and one asymptotic constant that conceptually relate to rates of rapid initial and slower, subsequent settling of sediment.
3. Coupled resuspension and consolidation tests for initial concentrations (C_0) comparable to fluid mud ($20\text{--}21 \text{ kg m}^{-3}$) showed that the shear stresses generating the highest turbidity peaks increased from ≤ 0.3 Pa after 2 weeks of consolidation to ≥ 0.45 Pa after 4 weeks of consolidation. This strengthening cannot be attributed solely to increasing sediment concentration during this relatively short period of time.
4. Comparison of these measured erosion shear stresses with bed shear stresses typical of coastal lakes and bays in the study area suggested that this degree of strengthening, if given time to occur, could increase the overall retention of fine sediments deposited on lake and bay floors.

Acknowledgements For financial support, the authors thank the Harrison Chair Endowment of the LSU Foundation, the LA-STEM Research Scholars Program funded by NSF, the Ronald E. McNair Research Scholars Program, LSU Chancellor's Student Aide and The Water Institute of the Gulf. For logistical support, we thank the Coastal Studies Field Support Group. Larry Sanford, Steve Suttles and Vincent Kelly helped develop and manufacture the Gust Erosion Microcosm System used in this study. We thank Dr. Tiffany Roberts for suggestions that were used to improve this manuscript. This article benefitted from the thoughtful assessments of one anonymous external reviewer and the journal editors.

References

- Amoudry LO, Souza AJ (2011) Deterministic coastal morphological and sediment transport modeling: a review and discussion. *Rev Geophys* 49, RG2002. doi:10.1029/2010RG000341
- Baker A, Henkel T, Boyd E, Lopez J (2011) Geomorphology and bald cypress restoration of the Caernarvon Delta near the Caernarvon Diversion, Southeast Louisiana. Lake Pontchartrain Basin Foundation, Coastal Sustainability Program. <http://www.saveourlake.org>. Accessed 1 Dec. 2013
- Blum MD, Roberts HH (2009) Drowning of the Mississippi Delta due to insufficient sediment supply and global sea-level rise. *Nature Geosci* 2:488–491. doi:10.1038/ngeo553
- Boudreau BP, Bennett RH (1999) New rheological and porosity equations for steady-state compaction. *Am J Sci* 299:517–528
- CWPPRA (2013) South Lake Lery Shoreline and Marsh Restoration Project Data. Coastal Wetlands Planning, Protection and Restoration Act. <http://lacoast.gov/reports/managers.asp?projectNumber=BS-16>. Accessed 27 Jan. 2014
- Dickhudt PJ, Friedrichs CT, Schaffner LC, Sanford LP (2009) Spatial and temporal variation in cohesive sediment erodibility in the York River estuary, eastern USA: a biologically influenced equilibrium modified by seasonal deposition. *Mar Geol* 267:128–140. doi:10.1016/j.margeo.2009.09.009
- Dickhudt PJ, Friedrichs CT, Sanford LP (2011) Mud matrix solids fraction and bed erodibility in the York River, USA, and other muddy

- environments. *Cont Shelf Res* 31(10S):S3–S13. doi:10.1016/j.csr.2010.02.008
- Fall K, Harris CK, Friedrichs CT, Rinehimer JP, Sherwood CR (2014) Model behavior and sensitivity in an application of the cohesive bed component of the community sediment transport modeling system for the York River Estuary, VA, USA. *J Mar Sci Eng* 2:413–436. doi:10.3390/jmse2020413
- Franks J, Stolz JF (2009) Flat-laminated microbial mat communities. *Earth-Sci Rev* 96:163–172. doi:10.1016/j.earscirev.2008.10.004
- Gong W, Shen J (2009) Response of sediment dynamics in the York River Estuary, USA to tropical cyclone Isabel of 2003. *Estuar Coastal Shelf Sci* 84(1):61–74. doi:10.1016/j.ecss.2009.06.004
- Green Eyes, LLC (2010) UMCES-Gust erosion microcosm system user manual. Easton, MD, pp 69
- Gust G, Muller V (1997) Interfacial hydrodynamics and entrainment functions of currently used erosion devices. In: Burt N, Parker R, Watts J (eds) *Cohesive sediments*. Wiley, Wallingford, pp 149–174
- Heiri O, Lotter AF, Lemcke G (2001) Loss on ignition as a method for estimating organic and carbonate content in sediments: reproducibility and comparability of results. *J Paleolimnol* 25:101–110. doi:10.1023/A:1008119611481
- Jepsen R, Roberts J, Lick W (1997) Effects of bulk density on sediment erosion rates. In: Kronvang B, Faganeli J, Ogrinc N (eds) *The interactions between sediments and water*. Springer, Heidelberg, pp 21–31
- Kineke GC, Sternberg RW, Trowbridge JH, Geyer WR (1996) Fluid-mud processes on the Amazon continental shelf. *Cont Shelf Res* 16:667–696. doi:10.1016/0278-4343(95)00050-X
- Kineke G, Higgins E, Hart K, Velasco D (2006) Fine-sediment transport associated with cold-front passages on the shallow shelf, Gulf of Mexico. *Cont Shelf Res* 26:2073–2091. doi:10.1016/j.csr.2006.07.023
- LA CPRA (2012) Louisiana's Comprehensive Master Plan for a Sustainable Coast. Coastal Protection and Restoration Authority. <http://www.coastalmasterplan.louisiana.gov/>. Accessed 1 Dec. 2013
- Lane RR, Day JW, Thibodeaux B (1999) Water quality analysis of a freshwater diversion at Caernarvon, Louisiana. *Estuaries* 22:327–336. doi:10.2307/1352988
- Law BA, Hill PS, Milligan TG, Curran KJ, Wiberg PL, Wheatcroft RA (2008) Size sorting of fine-grained sediments during erosion: results from the western Gulf of Lions. *Cont Shelf Res* 28:1935–1946. doi:10.1016/j.csr.2007.11.006
- Maa JP-Y, Sanford L, Halka JP (1998) Sediment resuspension characteristics in Baltimore Harbor, Maryland. *Mar Geol* 146:137–145. doi:10.1016/S0025-3227(97)00120-5
- McAnally WH, Friedrichs C, Hamilton D, Hayter E, Shrestha P, Rodriguez H, Sheremet A (2007) Management of fluid mud in estuaries, bays, and lakes. I: Present state of understanding on character and behavior. *J Hydraul Eng* 133(1):9–22
- Meselhe EA, Georgiou I, Allison MA, McCorquodale JA (2012) Numerical modeling of hydrodynamics and sediment transport in lower Mississippi at a proposed delta building diversion. *J Hydrol* 472(473):340–354. doi:10.1016/j.jhydrol.2012.09.043
- Moeller CC, Huh OK, Roberts H, Gumley LE, Menzel P (1993) Response of Louisiana coastal environments to a cold front passage. *J Coastal Res* 9:434–447
- Mulsow S, Boudreau BP, Smith JN (1998) Bioturbation and porosity gradients. *Limnol Oceanogr* 43:1–9. doi:10.4319/lo.1998.43.1.0001
- Neumeier U, Ferrarin C, Amos CL, Umgieser G, Li MZ (2008) Sedtrans05: an improved sediment-transport model for continental shelves and coastal waters with a new algorithm for cohesive sediments. *Comput Geosci* 34:1223–1242. doi:10.1016/j.cageo.2008.02.007
- Nittrouer JA, Allison MA, Campanella R (2008) Bedform transport rates for the lowermost Mississippi River. *J Geophys Res Earth Surf* 113, F03004. doi:10.1029/2007JF000795
- Palermo MR, Thackston EL (1988) Flocculent settling above zone settling interface. *J Environ Eng ASCE* 114:770–783. doi:10.1061/(ASCE)0733-9372(1988)114:4(770)
- Papenmeier S, Schrottke K, Bartholomä A, Flemming BW (2013) Sedimentological and rheological properties of the water–solid bed interface in the Weser and Ems estuaries, North Sea, Germany: implications for fluid mud classification. *J Coastal Res* 29:797–808. doi:10.2112/JCOASTRES-D-11-00144.1
- Rinehimer JP, Harris CK, Sherwood CR, Sanford LP (2008) Estimating cohesive sediment erosion and consolidation in a muddy tidally dominated environment: model behavior and sensitivity. In: *Proc 10th Int Conf Estuarine and Coastal Modeling*, pp 819–838. doi:10.1061/40990(324)44
- Roberts HH (1997) Dynamic changes of the Holocene Mississippi River delta plain: the delta cycle. *J Coastal Res* 13:605–627
- Sanford LP (2008) Modeling a dynamically varying mixed sediment bed with erosion, deposition, bioturbation, consolidation, and armoring. *Comput Geosci* 34:1263–1283. doi:10.1016/j.cageo.2008.02.011
- Schrottke K, Becker M, Bartholomä A, Flemming BW, Hebbeln D (2006) Fluid mud dynamics in the Weser estuary turbidity zone tracked by high-resolution side-scan sonar and parametric sub-bottom profiler. *Geo-Mar Lett* 26:185–198. doi:10.1007/s00367-006-0027-1
- Stevens AW, Wheatcroft RA, Wiberg PL (2007) Seabed properties and sediment erodibility along the western Adriatic margin, Italy. *Cont Shelf Res* 27:400–416. doi:10.1016/j.csr.2005.09.009
- Syvitski JPM, Kettner A, Overeem I, Hutton EWH, Hannon MT, Brakenridge GR, Day J, Vörösmarty C, Saito Y, Giosan L, Nicholls RJ (2009) Sinking deltas due to human activities. *Nature Geosci* 2:681–686. doi:10.1038/ngeo629
- Toorman EA (1996) Sedimentation and self-weight consolidation: general unifying theory. *Géotechnique* 46:103–113. doi:10.1680/geot.1996.46.1.103
- Toorman EA (1997) Modelling the thixotropic behaviour of dense cohesive sediment suspensions. *Rheologica Acta* 36(1):56–65
- Toorman EA, Berlamont JE (1993) Mathematical modeling of cohesive sediment settling and consolidation. In: Mehta AJ (ed) *Nearshore and estuarine cohesive sediment transport*. American Geophysical Union, Washington, DC, pp 167–184
- Turner TM (1996) *Fundamentals of hydraulic dredging*. ASCE Press, Reston, VA
- US-ACE (2002) *Coastal Engineering Manual*. Engineer Manual 1110-2-1100. US Army Corps of Engineers, Washington, DC
- US-ACE US-EPA (1998) *Evaluation of Dredged Material Proposed for Discharge in Waters of the U.S. – Testing Manual*. US Army Corps of Engineers and US Environmental Protection Agency, EPA-823-B-98-004. <http://water.epa.gov/type/oceb/oceandumping/dredgedmaterial/testing.cfm>. Accessed 29 Jan. 2014
- Wheelock K (2003) *Pulsed river flooding effects on sediment deposition in Breton Sound estuary, Louisiana*. MSc Thesis, Louisiana State University, Baton Rouge, LA
- Whitehouse R, Soulsby R, Roberts W, Mitchener H (2000) *Dynamics of estuarine muds: a manual for practical applications*. Thomas Telford, London
- Winterwerp JC (2002) On the flocculation and settling velocity of estuarine mud. *Cont Shelf Res* 22(9):1339–1360
- Winterwerp JC, Van Kesteren WGM (eds) (2004) *Introduction to the physics of cohesive sediment in the marine environment*. Elsevier, Amsterdam
- Wright LD (1995) *Morphodynamics of inner continental shelves*. CRC Press, Boca Raton, FL
- Xu K, Corbett D, Walsh J, Young D, Briggs K, Cartwright G, Friedrichs C, Harris C, Mickey R, Mitra S (2014) Seabed erodibility variations on the Louisiana continental shelf before and after the 2011 Mississippi River Flood. *Estuar Coastal Shelf Sci*. doi:10.1016/j.ecss.2014.09.002